**Materials Engineering and Technologies**

https://met.cultechpub.com/met

Cultech Publishing

*Article*

# Corn Silk-CuO Nanocomposites Synthesis for Effective Uptake of Cadmium from Aqueous Solution

**Chisom T. Okoye[*], Eze A. Ozukwe, Nwanneka G. Ezeokoye, Onyinyechukwu E. Udebuani, Chinonso D. Okoliko, Chinaza E. Nwoke, Odinaka A. Marcel**

Pure and Industrial Chemistry Department, Nnamdi Azikiwe University, Awka, Anambra, Nigeria

[*]Corresponding author: Chisom Theresa Okoye, umehchi871@gmail.com

**Abstract**

Toxic heavy metals have impacted a number of water bodies; wastewater treatment methods must be created to remove the pollutants from the aquatic environment. In this study, corn silk loaded with copper oxide was created and employed as a potential adsorbent for the uptake of cadmium ions, or Cd (II), from aqueous solution. Following the characterization of produced copper oxide nanoparticle loaded corn silk (CuO NPs/CS) using Fourier transform infrared spectroscopy (FTIR), scanning electron microscopy (SEM), and X-ray diffraction analysis (XRD), the adsorption operating variables (pH, dose, contact duration, temperature, and initial metal ion concentration) were calculated. At pH 6, contact period of 60 minutes, initial cadmium ion concentration of 20 mg/L, dosage of 0.5g, and monolayer absorption capabilities of 13.32 mg/g, the nano-adsorbent exhibited optimal adsorption. The experimental results showed a heterogeneous distribution of adsorbed metal ions on the CuO NPs/CS surface, with low error values and the best fit for the Freundlich isotherm. The uptake of Cd (II) onto the produced nanomaterial surface, which indicates a chemisorption process, is best explained by pseudo-second order kinetics. The intra-particle diffusion of Cd (II) ions to surface sites took place in three steps. Thermodynamic investigation revealed that the adsorption process happened spontaneously in an endothermic situation. After five successive cycles, the degree of reusability of CuO NPs/CS was evaluated, further demonstrating its potential for financial gain. In addition to pore filling, hydrogen bonding, and hydrophobic interactions, the characterisation and adsorption studies revealed the predominance of electrostatic attraction. The present work affirms that synthesized CuO NPs/CS could possess a promising application to cadmium ion removal from aqueous medium.

**Keywords**

Nano-adsorbent, Cadmium, Ciprofloxacin, Adsorption, Desorption

**Article History**

Received: 5 August 2025
Revised: 12 September 2025
Accepted: 16 September 2025
Available Online: 25 September 2025

## 1. Introduction

The dangerous effects of toxic heavy metal ions, can be harmful to aquatic species and the environment, making water body pollution a worldwide environmental phenomenon [1]. Because of their extreme persistence, poisonous metal ions can build up in internal organs and cause genotoxic, carcinogenic, and mutagenic health impacts on humans through the food chain [2-4]. Through a variety of industrial activities, including metal plating, smelting, phosphate fertilizer, sewage sludge, alloy industries, and refinement of cadmium-nickel batteries, dangerous metal ions like cadmium end up in the natural environment [5]. The accumulation of cadmium ion in polluted water can cause some physicochemical and neurological ailment in aquatic lives, hence, generating ecological disturbance and health threat to humans [6,7].

Recently, various wastewater treatment processes like membrane filtration, ion-exchange, electro-coagulation, adsorption, advanced oxidation processes, chemical precipitation, solvent extraction, photo catalysis, and microbial degradation have been proposed to decrease metallic ions in contaminated water [8]. Adsorption technique proves to be more effective and versatile for removal of cadmium ion in aqueous media. The adsorption method is often used as a treatment process due to its effective removal of toxic substances, cost advantages, provision of high-quality treated water when implemented with a well-designed plant system, and management of sludge disposal to the environment [9]. This phenomenon occurs at the surface level, where pollutants (adsorbates) adhere to the solid surface (adsorbent) due to attractive forces on the adsorbent's external surface. These forces cause adsorbate species to accumulate on that surface. Utilizing agricultural waste for adsorption offers a low-cost, renewable, readily available approach that contributes to alternative sustainability within the circular economy [10].

Nanotechnology seems to be a practical and promising option for the uptake of pollutants through the adsorption mechanism [11]. The ecofriendly green synthesis of nanoparticles via biological sources proves their efficiency in effluent treatment field due to their cost effectiveness, accessibility, and less toxicity to health [12]. Nanoparticles (NPs) are categorized by small sizes of about 1-100 nm that enable their high surface area to volume ratio to improve reactivity together with their solubility, mobility, interface effects and quantum features [13]. Because of their unique physical and chemical characteristics, nanomaterials have practical uses in the fields of biology, engineering, medicine, climate change, and the environment [14]. Through adsorption, nanoadsorbents can effectively remove both organic and inorganic pollutants from air and wastewater due to their high capacity [15]. The use of synthetic nanoparticles for the efficient adsorption of antibiotic medications and other contaminants has been demonstrated by recent research trends [16-19]. One of the significant transition metal oxide materials with monoclinic (CuO) structures that finds usage in a variety of applications is copper oxide nanoparticles [20,21].

Because of their narrow band gap, low cost, good textural qualities, high surface area, cytotoxicity, antibacterial activity, catalytic activity, abundance of active sites, and effective adsorption capacity, copper oxide nanoparticles have drawn a lot of attention [22].

Corn silk (CS) is a low-cost, fibrous, biodegradable, and non-toxic material. Its numerous chemical components, including proteins, polyphenols, steroids, and volatile oils, along with certain functional groups like hydroxyl, carboxyl, and carbonyl, make it perfect for adsorbing dyes and heavy metals [23]. Chemical pretreatment can further increase the adsorption capacity of this fibrous material, which is rich in functional groups and can probably be used as a sieve or filtration pad. Once more, Corn silk extract has demonstrated beneficial therapeutic effects for conditions like bladder infections, urinary system inflammation, prostate inflammation, and kidney stones. that are connected to the occurrence of bioactive components, particularly flavonoids and terpenoids [24]. Based on its chemical composition and functional groups that facilitate the exchange of hydrogen ions for other cations, it can be regarded as a potential bio-sorbent in acid-treated form for the removal of cadmium metal ions.

This study utilized copper oxide synthesized from corn silk as a promising nano-adsorbent for eliminating cadmium ions from aqueous solutions. The surface morphology and surface functional groups using scanning electron microscope (SEM) and Fourier transform infrared spectrometer (FT-IR) alongside with other chemical characterizations such as EDX and XRD. The adsorption effects of varying influencing parameters were estimated to determine equilibrium isotherm, kinetic and thermodynamics. This study also investigated the binding mechanistic process of cadmium ion onto prepared nanocomposite as well as the feasibility of regenerating the adsorbent through repeated adsorption–desorption experiments. This work's novelty lies in demonstrating the interaction effect and adsorption mechanism during equilibrium analysis concerning variation parameters, isotherm and kinetic modelling.

## 2. Materials and Methods

### 2.1 Synthesis of Copper Oxide Nanoparticles Impregnated Biomass

Similar methods for magnetite nanoparticles on Musa acuminata peel [16] and nickel oxide nanoparticle-loaded nanocellulose [25] were used to create adsorbent composites. By initially dissolving 5 g of $CuSO4.5H_2O$ individually in 100 ml of distilled water on a hot plate and stirring for 30 minutes at 30 °C to guarantee full dissolution of the salts, the nanocomposites were made by thermo-chemical precipitation process in solution. Following that, 10 g of the produced CS each were introduced to two distinct beakers of salt solutions while being continuously stirred for two hours. A few

drops of 0.5 M NaOH were then added, and the mixture was stirred for a further eight hours, until the pH reached 11. A color change from light blue to dark blue was observed. Subsequently, the mixtures underwent centrifugation at 4000 rpm for 2 hours. This was succeeded by rinsing with excess water until the pH reached 7.0, centrifugation, and drying in an oven at 70 °C for 24 hours. The dried composites were ground and sieved through a 100-µm mesh screen to produce copper oxide impregnated CS, referred to as CuO NPs/CS composite.

### 2.2 Characterization of the Prepared Nano-adsorbent

The FT-IR spectra of the acid-treated adsorbent were obtained using an FT-IR spectrometer (Shimadzu 8400s) and KBr pellets, with measurements taken in the range of 4000 to 400 $cm^{-1}$. The distribution of molecules in acid-treated adsorbent, along with its porosity, roughness, morphological features, and structure, was examined using a scanning electron microscope (PhenomWorld Eindhoven, Netherlands). The adsorbent's mineral phase and diffraction pattern were determined using an X-ray diffractometer (XRD- Rigaku D/MaxlllC, PW 1800).

### 2.3 Equilibrium Studies

Using a batch adsorption approach, the cadmium ion was adsorbed onto the CuO NPs/CS composite. Typically, a 1000 mg/L stock solution of the pollutants was made, and then the stock was serially diluted to concentrations ranging from 20 to 100 mg/L. After adding 0.10 g of the appropriate adsorbent to 10 mL of 55 mg/L pollutant solutions at pH 7.0, the mixture was ultrasonically sonicated for 60 min at 303 K room temperature before being filtered. AAS was used to determine the concentration of the contaminant that remained in solution following adsorption. The effect of adsorbent dosage (0.10–0.5 g), sonication time (20–60 min), pH (3–9) and temperature (303–343 K) were studied by varying the factor of interest while keeping the others constant at the optimum conditions. The filtrate was analyzed for Cd(II) concentration by AAS in accordance with standard procedures. Equations 1 and 2 were used to determine the values of qe (the amount of equilibrium adsorption) and %R (the percentage removal).

$$qe=\frac{(C_o-C_e)V}{M} \quad (1)$$

$$\%R=\frac{C_o-C_e}{C_o}\times 100 \quad (2)$$

The concentrations of Cd (II) in the liquid phase at the start and at equilibrium (mg/L) are denoted as Co and Ce, respectively, while V (L) and M (g) refer to the volume of the adsorbate solution and the mass of the adsorbent used. All experiments were carried out with three replicates. The linear forms of the adsorption isotherm (Langmuir, Freundlich, Temkin, Sips, and D-R) were modeled as illustrated below.

$$\frac{\boldsymbol{C_e}}{\boldsymbol{q_e}}=\frac{\boldsymbol{1}}{\boldsymbol{q_{mK_L}}}+\frac{\boldsymbol{C_e}}{\boldsymbol{q_m}} \quad (3)$$

$$\text{Log } q_e=\log K_F+\frac{1}{n}\log C_e \quad (4)$$

$$qe=B\ lnK_T+B\ lnC_e \quad (5)$$

$$ln\left(\frac{q_e}{q_{max}-q_e}\right)=\frac{1}{n}ln\ C_e+\ln K_S \quad (6)$$

$$\ln qe=\ln q_m-K_{DR}\varepsilon^2 \quad (7)$$

$$\varepsilon=RT\ln\left[1+\frac{1}{C_e}\right] \quad (7a)$$

$$E=\frac{1}{\sqrt{2K_{DR}}} \quad (7b)$$

where Ce represents the equilibrium adsorbate concentration (mg/L), $K_L$ denotes the Langmuir constant, qe indicates the amount of adsorbate per unit mass of adsorbent that has been adsorbed (mg/g), and qm is the maximum adsorption capacity (mg/g). The Freundlich constants $K_F$ and n indicate the capacity and intensity of adsorption, respectively. $K_T$ (L/mg) represented the equilibrium binding constant linked to the maximal binding energy, whereas B was the Temkin constant related to the heat of adsorption (kJ/mol). T (measured in Kelvin) is the absolute temperature, E (in kJ/mol) denotes the mean free energy of adsorption, R (8.314 J/mol·K) is the universal gas constant, ε represents the Polanyi potential, and $K_{DR}$ (in $mol^2/kJ^2$) is a constant indicating the mean adsorption energy. 1/n represents the Sips model exponent, while Ks denotes the Sips equilibrium constant (L/mg).

Kinetics (Pseudo-first, second order, and Elovich) studies were evaluated as shown in equations:

$$\log(qe-qt)=loq\ qe-\frac{K_1t}{2.303} \quad (8)$$

$$\frac{t}{qt}=\frac{1}{k_2qe^2}+\frac{t}{qe} \quad (9)$$

$$qt=\frac{1}{\beta}\ln\ (\alpha\beta)+\frac{1}{\beta}\ln(t) \quad (10)$$

Additionally, as shown by equations 16 and 17, experimental data were modeled using liquid film diffusion (LFD) and intraparticle diffusion (IPD) models to evaluate adsorption control.

$$qt = K_{id}t^{1/2} + C \quad (11)$$

$$\ln(1 - F) = -K_{LFD}t + C \quad (12)$$

$$F = \frac{[q_t]}{[q_e]} \quad (12a)$$

Where $qe$ and $qt$ represent the amount of compound adsorbed at equilibrium and at any time $t$ (mg/g); $k_1$ (min$^{-1}$), $k_2$ (g/mg min), $K_{id}$ (mg/g/min$^{1/2}$), and $K_{LFD}$ (min$^{-1}$) are the equilibrium rate constants of pseudo-first-order, second-order, intra-particle diffusion, and liquid film diffusion adsorption; C is the intercept of IPD and LFD equations; F describes the fractional attainment to equilibrium; α is the initial sorption rate (mg/g min) and β is a desorption constant.

### 2.4 Error Analysis

Three statistical error functions were used, as indicated by the following equations, to estimate a better fit or accuracy in identifying which of the isotherm models best describes the adsorption process.

$$\text{Sum square error (SSE)} = \sum_{i=1}^{n} (q_{e,cal} - q_{e,\exp})_i^2 \quad (13)$$

$$\text{Sum of absolute error (EABS)} = \sum_{i=1}^{n} \left| q_{e,exp} - q_{e,cal} \right| \quad (14)$$

$$\text{Chi-square test } (\chi^2) = \sum_{i=1}^{n} \frac{(q_{e,exp} - q_{e,cal})^2}{q_{e,exp}} \quad (15)$$

Where $q_{e,exp}$ is the experimental value while $q_{e,cal}$ is the calculated value from the isotherm models and n is the number of observations in the experiment.

### 2.5 Thermodynamic Study

To evaluate the process of cadmium ion, malachite green dye, and ciprofloxacin uptake from aqueous solution, as well as the feasibility and spontaneity of the adsorption process, which is highly reliant on the type of the adsorbent, the adsorption thermodynamic was evaluated. Adsorption of Cd (II) on CuO NPs/CS was studied thermodynamically at five different temperatures (303, 313, 323, 333, and 343K). The following equations were used for thermodynamic study.

$$\Delta G^o = -RTlnK_C = \Delta H^o - T\Delta S^o \quad (16)$$

$$lnK_C = -\left(\frac{\Delta H^o}{RT}\right) + \left(\frac{\Delta S^o}{R}\right) \quad (17)$$

$$lnK_C = \frac{q_e}{c_e} \quad (18)$$

Where $\Delta G°$ is change in standard Gibbs free energy, $R$ is a universal gas constant 8.314 J/ (mol. K), and $T$=Temperature, ΔH°, ΔG°, and ΔS° denotes change in enthalpy, free energy, entropy, respectively, and $K_C$ is adsorption thermodynamic equilibrium constant.

### 2.6 Desorption Studies

Experiments on desorption were conducted in a batch setup. After adding 500 mL of 200 mg/L Cd (II) solution to the CuO NPs/CS sample (0.5g), the suspensions were shaken for 120 min at room temperature (250 rpm), filtered through filter paper, and washed with deionized water. After that, 500 mL of 0.1mol/L $HNO_3$ in the beaker was mixed with Cd (II) loaded CuO NPs/CS separately, and the mixture was agitated for 120 min at room temperature (250 rpm). After passing through filter paper, the suspensions were rinsed, dried at 353K, and then utilized again for desorption investigations. To calculate the desorption efficiency, the adsorption-desorption tests were conducted five times. The desorption efficiency was computed using equation 19:

$$d_E = \frac{q_{de}}{q_{ad}} \times 100 \quad (19)$$

Where $d_E$ is the desorption efficiency (%), $q_{de}$ is the desorbed concentration and $q_{ad}$ signifies the adsorbed concentration of the target pollutant onto each adsorbent.

## 3 Results and Discussion

### 3.1 Nano-adsorbent Characterization

The SEM micrograph of the studied nano-adsorbent at different sizes suggests that the surfaces of the metal oxide-modified material are uneven and coarse, featuring numerous channels that provide binding sorption sites for cadmium ions, as illustrated in Figure 1a and 1b. The diffusion of the target pollutant molecules to and from the interior and

exterior of the adsorbents is allowed by these channels. The SEM image of the synthesized CuO NPs/CS indicates that the NPs were spherical in shape, with some particles showing signs of agglomeration.

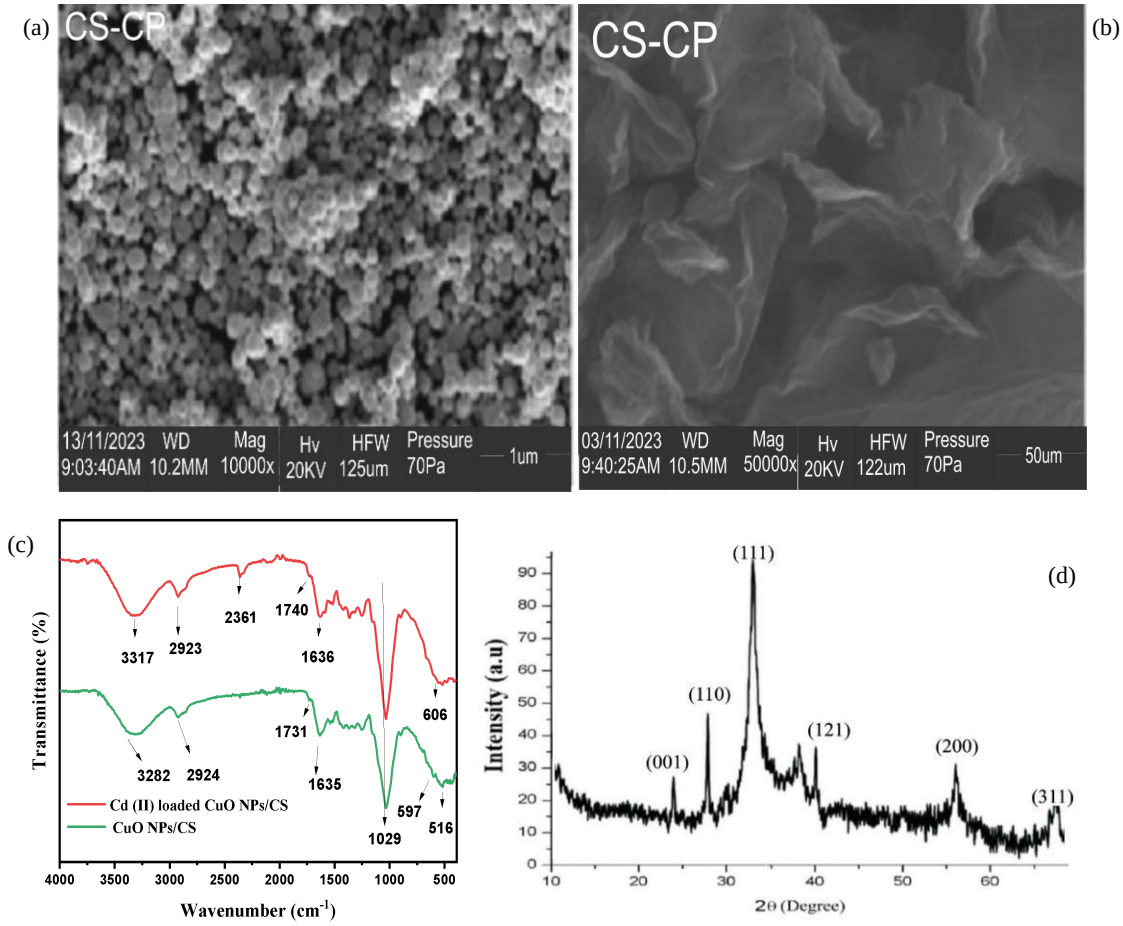


**Figure 1.** SEM Images of CuO NPs/CS (a) at 1µm, (b)50 µm, (c) FTIR Spectra and (d) XRD.

Figure 1c shows that the peaks at 3282, 2924, 1731, 1635, and 1029 $cm^{-1}$ are O-H, C-H, C=O, C=C, and C-O stretching bands characteristic of cellulose, lignin, and pectin found in the nano-adsorbent. A vibrational band at 597 $cm^{-1}$ is characteristic of the Cu-O functional group. The subsequent creation of Cu-O was validated by absorption peaks in the 500-700 $cm^{-1}$ range, as previously noted [26,27]. As noted once more, the wide and pronounced peaks at 516 $cm^{-1}$ were attributed to stretching vibrations of Cu-O, resulting from the copper oxide functional group.

Prajapati and Mondal [28] described a similar situation involving the adsorption of methylene blue using CuONPs, exhibiting a peak at 519 $cm^{-1}$ that suggested Cu-O bonding. Band shifts from (3282 to 3317 $cm^{-1}$), (2924 to 2923 $cm^{-1}$), (1731 to 1740 $cm^{-1}$), and (1635 to 1636 $cm^{-1}$) following the adsorption of cadmium ions suggested the usage of O-H, C-H, C=O, and C=C functional groups for the intake of metal ions. The C-O vibration of the adsorbents is not significantly impacted by the uptake of cadmium metal ions since the values stay constant during the sorption process. Again, the presence of vibrational band at 2361 $cm^{-1}$ for alkyne group in cadmium loaded metal oxide spectrum and insignificant in CuO NPs/CS spectra that contributed to interaction of surface properties of the nanocomposites to facilitate cadmium ion.

As seen in Figure 1d, the phases and crystalline nature of the impregnated corn silk nano-sorbent were determined using its XRD spectrum. The diffraction peaks at 2 theta values of 23.22°, 28.47°, 33.22°, 40.22°, 52.21°, and 68.02° correspond to the monoclinic crystalline planes of CuO NPs/CS that are indexed as (001), (110), (111), (121), (200), and (300). Some of the indexed planes such as (110), (111) and (200) was as well observed in synthesized study carried out by Chowdhury et al. [29]. A study on the antibacterial properties of CuO nanoparticle-mediated Curcuma longa revealed a high peak at 43.30° with crystalline plane (111)[30]. According to the Debye-Scherrer formula ($D=k\lambda/\beta\cos\theta$), which shows the sequential creation of the target metallic oxide nanoparticles for adsorption effectiveness, the average crystalline sizes for CuO NPs/CS were determined to be 18.1 nm.

The energy dispersive X-ray (EDX) analysis was determined to examine the chemical composition present in the adsorbent's surface as shown in Table 1. The major constituents of the raw adsorbents are silicon, oxygen, carbon, aluminum, silver, calcium and iron with average weight composition ranging from 0.12 to 40.50% with higher contents of C, Al, Si, and Ag elements. The presence of Al, K and Ca indicates the mineral composition of the unmodified adsorbents. After the addition of CuO to the native adsorbent, copper was also found among the elements. This

apparently confirms the successful impregnation of CuO NPs onto corn silk. The carbon component of the nano-adsorbents was acquired from the bio-based components of the loaded plants.

**Table 1.** Elemental analysis of CuO NPs/CS.

| C | Al | Si | Ca | Na | Mg | Fe | Ag | Mn | O | Cu |
|---|---|---|---|---|---|---|---|---|---|---|
| 13.24 | 15.30 | 40.50 | 3.22 | 1.22 | 1.30 | 5.70 | 15.20 | 0.12 | 4.20 | 10.7 |

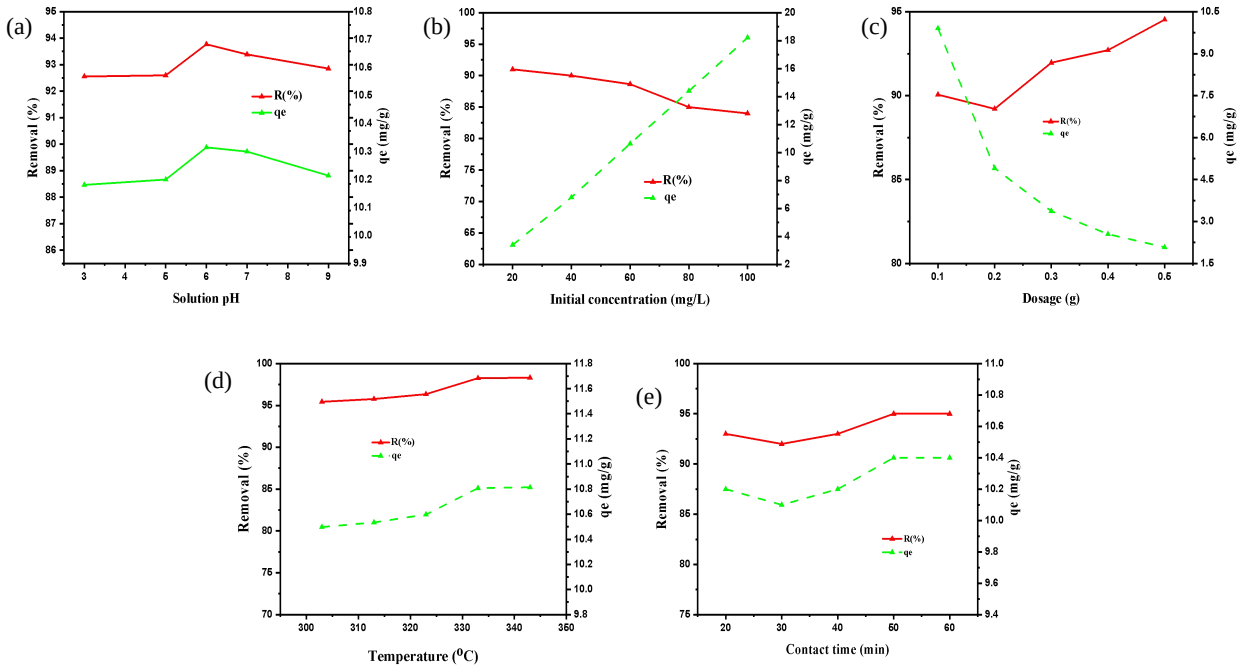


**Figure 2.** Effect of (a) pH, (b) Concentration, (c) Dosage, (d) Temperature and (e) Contact Time on Adsorption of Cd (II) onto CuO NPs/CS.

### 3.2 Effect of Solution pH

Since the pH of the aqueous solution influences the adsorbent's surface charge and the ionization pattern of the adsorbate species, it is the most significant factor governing the adsorption process of the investigated pollutant onto suspended particles [31]. Figure 2a shows that both adsorption capacity and removal efficiency for Cd (II) increase with increasing pH, with higher absorption at pH 6. When the pH of the metal ion solution increases, the functional groups on the adsorbents' surfaces become deprotonated thereby increasing the quantity of hydronium ions in the solution. This enable the attraction and adsorption of positively charged cadmium ions with maximum absorption capacity. With the increase in pH, the number of negatively charged surface sites on the nano-adsorbent studied increased, thereby enhancing the electrostatic interaction between the metal ion and the adsorbent, which is a primary mechanism [32]. At lower pH, the electrostatic repulsion between the protonated surface and the pollutant species hindered further adsorption. At pH 6, which is between the $pKa_1$ (5.9) and $pKa_2$ (8.9) constants [33], a higher adsorption capacity was achieved.

### 3.3 Effect of Metal ion Concentration

The mechanism of pollutant uptake relies on the initial concentration of the pollutant: at lower concentrations, adsorbate species are attached to specific binding sites, while at higher concentrations, the adsorption yield is low due to these sites being filled. As illustrated in Figure 2b, the bio-sorbent capacity for Cd (II) rose from 3.39 to 18.22 mg/g when the initial concentration was raised from 20 to 100 mg/L. At elevated concentrations, the driving force of the adsorbate species from high collision to overcome mass transfer resistance of the pollutants between the aqueous and adsorbent solid phase until saturation was enhanced [34]. At 20 mg/L, the highest uptake of Cd(II) was recorded at a percentage of 91.1%. This is as a result of available active sites on the nano-adsorbent during the early stages of adsorption. Presumable observations on cadmium ion adsorption were reported using other adsorbing materials [35].

### 3.4 Effect of Dosage

As shown in Figure 2c, the adsorption absorption capacity of the cadmium ion drops dramatically from 9.9 to 2.0 mg/g as the dosage of the nano-adsorbent increases. The decrease in the adsorption capacity values of the corresponding adsorbent was caused by the remaining unsaturated binding sites and an excess of adsorbent for the uptake of metal ions

during the adsorption process [36]. Additionally, the decrease in adsorption capacity can be linked to particle aggregation from higher adsorbent doses, which would lead to a smaller surface area and a shorter diffusion path for adsorbate species to go through inside the nano-adsorbent [37]. The removal of Cd (II) increased from 90.1% to 94.5% with the increase in CuO NPs/CS dosage. This indicates that the uptake capacity is indicative of the properties of the adsorbent material, whereas the percentage removal relates to the adsorbate or contaminant present in solution. From the findings, an adsorbent dosage of 0.5g yielded the highest observed effectiveness in removing target pollutants. The enhanced effectiveness of removal can be ascribed to the increase in surface area and the number of accessible active sites that occurs with a higher adsorbent dose, as these are essential for high levels of adsorption.

### 3.5 Effect of Temperature

The effect of temperature on the adsorption efficiency of CuO NPs/CS for cadmium metal ions was examined, as depicted in Figure 2d. The cadmium ion's bio-sorption capacity and adsorption removal efficiency rose with increasing temperature, likely due to heightened surface activity. This suggests that the interaction between the cadmium metal ion and the nano-adsorbent is an endothermic process, with adsorption being enhanced at elevated temperatures. The removal efficiency rises with temperature, but at 343K it decreased. This might result from a reduction in the thickness of the boundary layer at that temperature, which allowed Cd (II) ions to escape from the adsorbent surface [38]. Because more adsorbing pore sites are created or the volume of inner pores is increased for more interaction with the target pollutant, biosorption efficiency is extremely noticeable in produced nanocomposites [39]. Additionally, as the temperature rises, the aqueous solution's decreased viscosity may make it easier for Cd (II) particles to migrate toward the adsorbents' surface sites, which could result in a high rate of collision between the adsorbents and the adsorbate molecules [40].

### 3.6 Effect of Contact Time

Another crucial factor in the adsorption process to achieve equilibrium is the impact of contact time. It was shown that the absorption capability of the CuO NPs/CS nano-adsorbent rose from 10.2 to 10.4 mg/g when the contact period with metal ions increased from 20 to 60 minutes. The percentage Cd (II) removal for the corresponding materials in Figure 2e increased similarly, from 92.6 to 94.5%. As time increased, the adsorption capacity and removal efficiency rose in a sequential manner. After 50 minutes of treatment, adsorption equilibrium was reached. Rapid adsorption was regulated by a diffusion mechanism from the bulk to the surface of the adsorbent.

From 40 to 60 min, a rapid adsorption rate was achieved due to the presence of unsaturated vacant sites before equilibrium was reached. In summary, the surface of the nanocomposite adsorbent shows a greater affinity for cadmium metal ions based on the higher percentage removal. Higher Cd (II) removal effectiveness (> 80%) of three local fruit peel bio-sorbents was documented by (Amnuay *et al*. [41]).

### 3.7 Equilibrium Isotherm

To assess the relevance of the Langmuir, Freundlich, Temkin, Sips, and D-R isotherms for the adsorption of cadmium metal ions onto CuO NPs/CS nano-adsorbent at various concentrations, linear representations of the selected isotherms were created (Figures 3), along with calculations of isotherm parameters and estimated error metrics (Table 2). Furthermore, standard error analyses were conducted to identify the most appropriate isotherm model for characterizing the adsorption process. The Langmuir isotherm assumes a monolayer and uniform distribution of surface sites for the target pollutant, with equal energy on the adsorbent surface. In contrast, the Freundlich isotherm features a non-uniform and heterogeneous distribution of adsorption sites with varying affinities [42].

The Sips isotherm results from the limiting behavior of Freundlich and Langmuir. Temkin indicates that the adsorbent and adsorbate have a high electrostatic connection [43]. The D-R model addresses the energy involved in the adsorption process as well as the porous nature of the adsorbents. The table shows that for cadmium ion sorption, the Langmuir, Freundlich, and D-R models have higher regression values than the others. With lower examined error functions and higher correlation regression values ($R^2$>0.9), the isotherm data of cadmium metal ion equilibrium bio-sorption demonstrated a satisfactory match to the Freundlich model. CuO NPs/CS have a monolayer adsorption capability of 13.32 mg/g for Cd (II). This demonstrated that the pollutant ions and the active binding site on the homogenous surface of the nano-adsorbent had a monolayer adsorption mechanism [44]. The adsorption of Cd (II) on CuO NPs/CS using the Langmuir isotherm model produced a favorable coefficient value, with mean separation factor ($R_L$) parameters falling between 0 and 1, indicating a good adsorption process. Accordingly, the generated adsorbents would need fewer steps in an industrial operating process to achieve high Cd (II) uptake. A successful adsorption process is indicated by values for metal uptake in the range of 0 to 10 for the Freundlich isotherm n parameter. For the investigated adsorbate uptake, the Sips isotherm did not provide an acceptable adsorption fit. Compared to other tested isotherms with higher values of determined statistical error functions, the model exhibited a low regression coefficient ($R^2$<0.9). While calculating 1/n for Cd (II) ion, the Sips exponent n was determined to be under one, indicating Freundlich isotherm behavior. The D-R isotherm model was applied to equilibrium data to distinguish between chemical and physical adsorption on heterogeneous surfaces. According to the E parameter, physical adsorption is indicated by values between 0 and 8

kJ/mol, while chemical adsorption corresponds to values between 8 and 16 kJ/mol [45]. The E value obtained in this study (0.350 kJ/mol) suggests that bio-sorption occurred via a physical process.

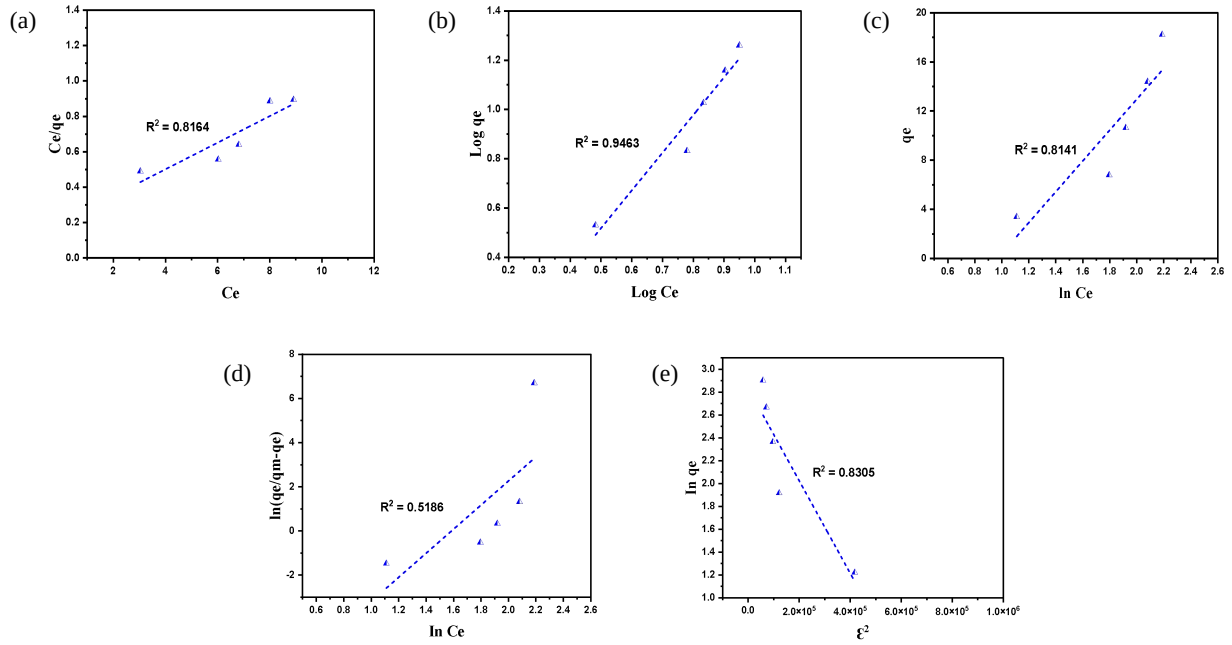


**Figure 3.** (a) Langmuir, (b) Freundlich, (c) Temkin, (d) Sips and (e) Dubinin-Radushkevich plots for Cd (II) uptake onto CuO NPs/CS.

**Table 2.** Isotherm parameters for the uptake of Cd (II) on CuO NPs/CS.

| Models | Parameters | Cadmium |
|---|---|---|
| **Langmuir** | $K_L$ (L/mg) | 0.374 |
| | $q_m$ (mg/g) | 13.32 |
| | $R^2$ | 0.8164 |
| | $R_L$ | 0.056 |
| | SSE | 103.714 |
| | EABS | 19.577 |
| | $X^2$ | 9.828 |
| **Freundlich** | $K_F$ (L/g) | 0.566 |
| | $N$ | 0.653 |
| | $R^2$ | 0.9463 |
| | SSE | 9.248 |
| | EABS | 5.210 |
| | $X^2$ | 0.922 |
| **Temkin** | $K_T$ (L/g) | 0.380 |
| | $B$ (kJ/mol) | 12.56 |
| | $R^2$ | 0.8141 |
| | SSE | 25.814 |
| | EABS | 9.825 |
| | $X^2$ | 3.296 |
| **Sips** | $N$ | 5.45 |
| | $q_m$ (mg/g) | 18.24 |
| | $K_S$ (L/mg) | 0.0002 |
| | $R^2$ | 0.5186 |
| | SSE | 87.380 |
| | EABS | 17.552 |
| | $X^2$ | 11.563 |
| **D-R** | $K_{DR}$ ($mol^2/kJ^2$) | 4.08E-6 |
| | $q_m$ (mg/g) | 17.02 |
| | $E$ (kJ/mol) | 0.350 |
| | $R^2$ | 0.8305 |
| | SSE | 39.354 |
| | EABS | 11.176 |
| | $X^2$ | 3.424 |

### 3.8 Kinetic Evaluation

The rate at which Cd (II) binds to the prepared nano-adsorbent and the mechanism of the adsorption process were estimated by investigating the rate of adsorption kinetics through time-dependent analysis, as shown in Figure 4 and Table 3. By taking kinetic models into consideration, one can predict the likely reaction mechanism, pathway, and duration for achieving adsorption equilibrium. These predictions may provide a theoretical foundation for the development and use of adsorbents in industrial contexts [46]. The experimental data obtained from the study of kinetics was evaluated using Pseudo-first order, Pseudo-second order, Elovich, Intra-particle diffusion, and Liquid film diffusion models respectively. When compared to pseudo-first order and elovich models, the bio-sorption operation for the uptake of cadmium ions showed good agreement with the pseudo-second order model based on a higher $R^2$ value, a lower residual sum square, and a calculated qe that was closer to the experimental one. This suggested that the mechanism of chemisorption, which involves the exchange of electrons between the cadmium ions and the binding sites of the adsorbent particles, actually controlled the kinetic model [47].

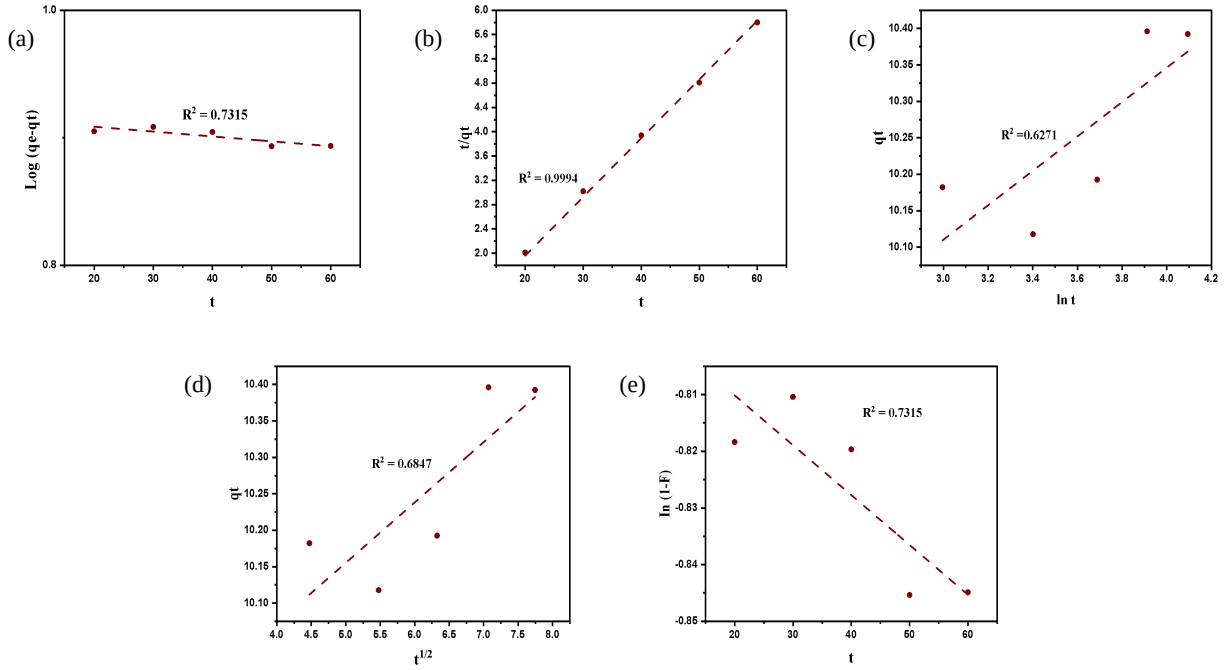


**Figure 4.** (a) Pseudo-first Order (b) Pseudo-second Order, (c) Elovich, (d) Intraparticle Diffusion and (e) Liquid Film Diffusion Plots for Cd (II) Uptake.

**Table 3.** Kinetic parameters for the adsorptive removal of cadmium ion

| Models | Parameters | Cadmium |
|---|---|---|
| | $qe_{exp}$ (mg/g) | 18.22 |
| **Pseudo-first order** | $k_1$ ($min^{-1}$) | 8.80E-04 |
| | $qe_{cal}$ (mg/g) | 8.25 |
| | $R^2$ | 0.7315 |
| | RSS | 5.36E-05 |
| **Pseudo-second order** | $k_2$ (mg/g.min) | 0.05 |
| | $qe_{cal}$ (mg/g) | 10.67 |
| | $R^2$ | 0.9994 |
| | RSS | 0.005 |
| **Elovich** | $\alpha$ ($g.min^2/mg$) | 4.76E16 |
| | $\beta$ (g.min/mg) | 4.24 |
| | $R^2$ | 0.6271 |
| | RSS | 0.025 |
| **Intraparticle diffusion** | $K_{id}$ ($mg/g/min^{1/2}$) | 0.083 |
| | $C$ | 9.741 |
| | $R^2$ | 0.6847 |
| | RSS | 0.021 |
| **Liquid film diffusion** | $K_{fd}$ | 8.80E-04 |
| | $D$ | 0.793 |
| | $R^2$ | 0.7315 |
| | RSS | 2.84E-04 |

The diffusion mechanism of the adsorption process was confirmed using the intra-particle diffusion and liquid film diffusion models. The involvement of boundary layer penetration in the adsorption process was confirmed by the absence of passing through the IPD and LFD linear diagrams from the origin in this study. Based on the plots, we may conclude that the full time range plot is nonlinear and displays multi-linearity. Thus, the rate is not determined by either LFD or IPD alone; instead, LFD and IPD collaborate to regulate the elimination of Cd (II) from water using nano-adsorbent. However, as the adsorbent thickness (C) in the IPD model was greater than zero for all initial Cd (II) concentrations, it can be concluded that this model does more than merely control each stage of the pollutants' adsorption process. As a result, the adsorption process was affected by other processes like complexes that would control the rate of adsorption and the thickness of the boundary layer [48].

### 3.9 Thermodynamic Study

The adsorption of cadmium ions onto the prepared nano-adsorbent was studied at temperatures ranging from 303 to 343 K to ascertain thermodynamic parameters and understand the influence of the adsorption mechanism on temperature variations. The negative ΔG° values (Table 4) indicate that Cd (II) was spontaneously adsorbed onto the produced adsorbent across all tested temperatures. The estimated entropy value ($\Delta S^o$) for the adsorption of Cd (II) ions on CuO NPs/CS was 94.71 J/mol·K, indicating an increase in the degree of randomness of CuO NPs/CS-Cd ions during the adsorption process. The successful adsorption of Cd (II) had a positive enthalpy value of 25.450 kJ/mol, indicating that the nano remediation process was endothermic. Additionally, a high regression value of 0.8570 was attained. In all temperatures examined, it was shown that impregnating maize silk with copper oxide nanoparticles enhanced the spontaneity of the cadmium ion adsorption process. Takdastan et al. [48] reported a positive entropy value on removal of cadmium ion using oak trash.

**Table 4.** Thermodynamic analysis of Cd (II) adsorption onto CuO NPs/CS

| Pollutants | Temperature | $\Delta G^o$ (kJ/mol) | $\Delta H^o$ (kJ/mol) | $\Delta S^o$ (J/mol.K) | $R^2$ |
|---|---|---|---|---|---|
| | 303K | -3.60 | 25.450 | 94.71 | 0.8570 |
| | 313K | -3.930 | | | |
| **Cd (II)** | 323K | -4.462 | | | |
| | 333K | -6.709 | | | |
| | 343K | -7.006 | | | |

### 3.10 Desorption Study

Figure 5 shows the error-barred results of the desorption analysis of produced CuO NPs/CS for the removal of cadmium ions. The suggested adsorbent should exhibit good operational adsorption and regeneration behavior for improved industrial use, sustainability, and economic viability [21][49]. In addition, for economic friendly process, the eluting agent used should be readily available and less toxic to the bio-sorbent. In view of that, nitric acid was used as a diluent for the desorption study and the nanomaterial showed a high stability for the tested five runs with high removal efficiency. The removal percentage dropped from 98.36% to 72.88% for the repeated cycles. The rate at which Cd (II) was adsorbed onto CuO NPs/CS nanocomposite showed a gradual and considerable decline with each successive cycle. The reduction in the adsorption rate may be due to several factors: the nano-adsorbent materials losing weight, not all functional groups being fully desorbed prior to reuse, and a cumulative effect from repeated treatments during the elution process. These factors can result in metal ion particles depositing on the adsorbent surface and blocking its pores [16][50]. Regardless of these factors, the CuO NPs/CS nano-adsorbent demonstrated an effective potential for recycling.

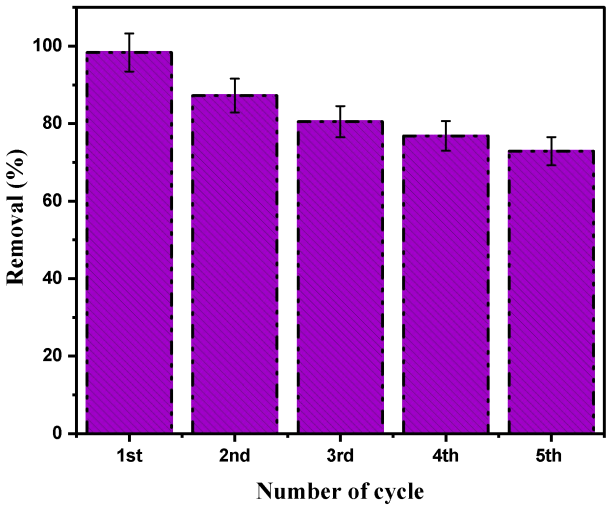


**Figure 5.** Reusability of CuO NPs/CS for Uptake of Cadmium Ion.

### 3.11 Possible Mechanism of Adsorption

In order to describe the adsorption operation as regards to treatment of cadmium metal ion contaminated industrial effluents, you have to understand the serial mechanism involved in the removal process. Carbonyl, carboxyl, hydroxyl and ether groups present on the surface of lignin, cellulose and hemicellulose were verified as the active binding sites on corn silk matrix and after CuO NPs impregnation for $Cd^{2+}$ sequestration in accordance to FTIR analysis. The elucidation from FTIR analysis of the adsorbents before and after Cd (II) adsorption provided an insight on the mechanism of target pollutant uptake onto CuO NPs/CS nanocomposite. It has been stated that the presence of noted functional moieties together with the electrostatic and coordination interaction involved in adsorption mechanism are attributed to the retention of positively charged $Cd^{2+}$ ion onto studied nano-adsorbent surfaces. From the displayed SEM images, there are presence of numerous pores for effective attachment and uptake of cadmium ion from aqueous media. The impregnation of CuO nanoparticles actually improved the active surface sites of the native adsorbent. For porous adsorbent materials, pore filling is also a typical mechanism that occurs allowing for improved uptake. Therefore, based on the characterizations and equilibrium tests carried out, the probable adsorption mechanism for effective sequestration cadmium ion from aqeous solution are pore filling, electrostatic attractions, hydrogen bonding and hydrophobic interactions.

## 4 Conclusion

The synthesis of copper oxide nanoparticle-impregnated corn silk was conducted in this study to improve its ability to adsorb cadmium ions. Further characterization of the nano-adsorbent was conducted using SEM, FTIR, and XRD analyses to potentially confirm the process of removing target pollutants. The maximum adsorption capacity achieved by the prepared CuO NPs/CS for Cd (II) was 13.32 mg/g. Through examination of adsorption factors, optimal conditions were found to be a pH of 6, contact time of 60 minutes, metal ion concentration of 20 mg/L, temperature of 343K and adsorbent dose of 0.5g. The experimental data on cadmium ion adsorption were found to be compatible with the Freundlich model. The adsorption of Cd (II) ion onto prepared CuO NPs/CS nano-adsorbent was followed by the pseudo-second order reaction. The produced nano-adsorbent adsorption of the Cd (II) ion was demonstrated by adsorption thermodynamics to form a spontaneous endothermic reaction mechanism with an increase in degree of unpredictability. In order to maximize economic efficiency, the nano-adsorbent can be recycled and used five times to sequester the investigated contaminant. The mechanisms of pore filling, electrostatic attraction, hydrogen bonding, and hydrophobic interactions were primarily responsible for the effective adsorption process. The analysis and extract findings demonstrated the possible use of the produced CuO NPs/CS nano-adsorbent for the treatment of wastewater containing cadmium ions.

### Funding

The authors received no funding for this research work.

### Conflict of interest

The authors declare no financial competing interest

### Generative AI statement

The authors declare that no Gen AI was used in the creation of this manuscript.

### References

[1] Sasmal D, Banerjee S, Senapati S, Tripathy T. Effective removal of $Th^{4+}$, $Pb^{2+}$, $Cd^{2+}$, malachite green, methyl violet and methylene blue from their aqueous solution by amylopectin dialdehyde-Schiff base. Journal of Environmental Chemical Engineering, 2020, 8(3), 103741. DOI: 10.1016/j.jece.2020.103741

[2] Murthy TPK, Gowrishankar BS, Prabha, MNC, Kruthi M, Krishna RH. Studies on batch adsorptive removal of malachite green from synthetic wastewater using acid treated coffee husk: Equilibrium, kinetics and thermodynamic studies. Microchemical, 2019, 146, 192-201. DOI: 10.1016/j.microc.2018.12.067

[3] Umeh C, Asegbeloyin JN, Akpomie KG, Oyeka EE, Ochonogor AE. Adsorption properties of tropical soils from Awka North Anambra Nigeria for lead and cadmium ions from aqueous media. Chemistry Africa, 2020, 3(1), 199-210. DOI: 10.1007/s42250-019-00109-3

[4] Umeh CT, Nduka JK, Akpomie KG. Kinetics and isotherm modeling of Pb(II) and Cd(II) sequestration from polluted water onto tropical ultisol obtained from Enugu Nigeria. Applied Water Science, 2021, 11(4), 65. DOI: 10.1007/s13201-021-01402-8

[5] Simić M, Petrović J, Šoštarić T, Ercegović M, Milojković J, Lopičić Z, et al. Mechanism assessment and differences of cadmium adsorption on raw and alkali-modified agricultural waste. Processes, 2022, 10(10), 1957. DOI: 10.3390/pr10101957

[6] Saeidi N, Parvini M, Niavarani Z. High surface area and mesoporous graphene/activated carbon composite for adsorption of Pb (II) from wastewater. Journal of Environmental Chemical Engineering, 2015, 3(4), 2697-2706. DOI: 10.1016/j.jece.2015.09.023

[7] Sikder MT, Jakariya M, Rahman MM, Fujita S, Saito T, Kurasaki M. Facile synthesis, characterization, and adsorption properties of Cd (II) from aqueous solution using β-cyclodextrin polymer impregnated in functionalized chitosan beads as a novel adsorbent. Journal of Environmental Chemical Engineering, 2017, 5(4), 3395-3404. DOI: 10.1016/j.jece.2017.06.007
[8] de lima LS, Quinaia SP, Melquiades FL, de Biasi GEV, Garacia JR. Characterization of activated carbons from different sources and the simultaneous adsorption of Cu, Cr, and Zn from metallurgic effluent. Separation and Purification Technology, 2014, 122, 421-430. DOI: 10.1016/j.seppur.2013.11.034
[9] Elamin MR, Abdulkhair BY, Algethami FK, Khezami L. Linear and nonlinear investigations for the adsorption of paracetamol and metformin from water on acid-treated clay. Scientific Reports, 2021, 11(1), 13606. DOI: 10.1038/s41598-021-93040-y
[10] Elgarahy AM, Elwakeel KZ, Mohammad SH, Elshoubaky GA. A critical review of biosorption of dyes, heavy metals and metalloids from wastewater as an efficient and green process. Cleaner Engineering and Technology, 2021, 4, 100209. DOI: 10.1016/j.clet.2021.100209
[11] Sassa-deepaeng T, Yodthong W, Khumpirapang N, Anuchapreeda S, Okonogi S. Effects of plant-based copper nanoparticles on the elimination of ciprofloxacin. Drug Discoveries & Therapeutics, 2023, 17(5), 320-327. DOI: 10.5582/ddt.2023.01057
[12] Khan SA, Ismail M, Anwar Y, Farooq A, Al Johny BO, Akhtar K, et al. A highly efficient and multifunctional biomass supporting Ag, Ni, and Cu nanoparticles through wetness impregnation for environmental remediation. Green Processing and Synthesis, 2019, 8, 309-319. DOI: 10.1515/gps-2018-0101
[13] Eid AM, Fouda A, Hassan SED, Hamza MF, Alharbi NK, Elkelish A, et al. Plant-based copper oxide nanoparticles; biosynthesis, characterization, antibacterial activity, tanning wastewater treatment, and heavy metals sorption. Catalysts, 2023, 13(2), 348. DOI: 10.3390/catal13020348
[14] Hamza MF, Abdel-Rahman AAH, Hawata MA, El Araby R, Guibal E, Fouda A, et al. Functionalization of magnetic chitosan microparticles—Comparison of trione and trithione grafting for enhanced silver sorption and application to metal recovery from waste X-ray photographic films. Journal of Environmental Chemical Engineering, 2022, 10(3), 107939. DOI: 10.1016/j.jece.2022.107939
[15] Osagie C, Othmani A, Ghosh S, Malloum A, KashitarashEsfahani Z, Ahmadi S. Dyes adsorption from aqueous media through the nanotechnology: a review. Journal of Materials Research and Technology, 2021, 14, 2195-2218. DOI: 10.1016/j.jmrt.2021.07.085.
[16] Akpomie KG, Conradie J. Efficient synthesis of magnetic nanoparticle-Musa acuminata peel composite for the adsorption of anionic dye. Arabian Journal of Chemistry, 2020, 13(9), 7115-7131. DOI: 10.1016/j.arabjc.2020.07.017
[17] Chowdhury A, Kumari S, Khan AA, Chandra MR, Hussain S. Activated carbon loaded with Ni-Co-S nanoparticle for superior adsorption capacity of antibiotics and dye from wastewater: kinetics and isotherms. Colloids and Surfaces A: Physicochemical and Engineering Aspects, 2020, 611, 125868. DOI: 10.1016/j.colsurfa.2020.125868
[18] Gupta VK, Arunima Nayak A. Cadmium removal and recovery from aqueous solutions by novel adsorbents prepared from orange peel and $Fe_2O_3$ nanoparticles. Chemical Engineering Journal, 2012, 180, 81-90. DOI: 10.1016/j.cej.2011.11.006
[19] Al-Musawi TJ, Mahvi AH, Khatibi AD, Balarak D. Effective adsorption of ciprofloxacin antibiotic using powdered activated carbon magnetized by iron (III) oxide magnetic nanoparticles. Journal of Porous Materials, 2021, 28(3), 835-852. DOI: 10.1007/s10934-021-01039-7
[20] Anand GT, Nithiyavathia R, Ramesha R, Sundarama SJ, Kaviyarasu K. Structural and optical properties of nickel oxide nanoparticles: Investigation of antimicrobial applications. Surfaces and Interfaces, 2020, 18, 100460. DOI: 10.1016/j.surfin.2020.100460
[21] Akpomie KG, Conradie J. Efficient adsorptive removal of paracetamol and thiazolyl blue from polluted water onto biosynthesized copper oxide nanoparticles. Scientific Reports, 2023, 13(1), 859. DOI: 10.1038/s41598-023-28122-0
[22] Rather MY, Sundarapandian S. Facile green synthesis of copper oxide nanoparticles and their rhodamine-b dye adsorption property. Journal of Cluster Science, 2022, 33(3), 925-933. DOI: 10.1007/s10876-021-02025-4
[23] Kalantar Z, Nasab SG. Modeling and optimizing Cd(II) ions adsorption onto Corn Silk/Zeolite-Y composite from industrial effluents applying response surface methodology: isotherm, kinetic, and reusability studies. Journal of the Iranian Chemical Society, 2022, 19(10), 4209-4221. DOI: 10.1007/s13738-022-02594-9
[24] Gan D, Huang Q, Dou J, Huang H, Chen J, Liu M, et al. Bioinspired functionalization of MXenes ($Ti_3C_2TX$) with amino acids for efficient removal of heavy metal ions. Applied Surface Science, 2020, 504, 144603. DOI: 10.1016/j.apsusc.2019.144603.
[25] Mohammed KS, Atlabachew M, Abdu B, Desalew AA. A nanocellulose from sugarcane bagasse as a template for nickel oxide nanoparticles for removal of organic dyes from aqueous solution[J]. Scientific Reports, 2024, 14(1), 31684. DOI: 10.1038/s41598-024-81403-0
[26] Alhalili Z. Green synthesis of copper oxide nanoparticles CuO NPs from Eucalyptus globoulus leaf extract: Adsorption and design of experiments. Arabian Journal of Chemistry, 2022, 15, 103739. DOI: 10.1016/j.arabjc.2022.103739
[27] Al-Qasmi N. Facial eco-friendly synthesis of copper oxide nanoparticles using chia seeds extract and evaluation of its electrochemical activity. Processes, 2021, 9(11), 2027. DOI: 10.3390/pr9112027
[28] Prajapati AK, Mondal MK. Comprehensive kinetic and mass transfer modeling for methylene blue dye adsorption onto CuO nanoparticles loaded on nanoporous activated carbon prepared from waste coconut shell. Journal of Molecular Liquids, 2020, 307, 112949. DOI: 10.1016/j.molliq.2020.112949
[29] Chowdhury R, Khan A, Rashid MH. Green synthesis of CuO nanoparticles using Lantana camara flower extract and their potential catalytic activity towards the aza-Michael reaction. RSC Advances, 2020, 10(24), 14374-14385. DOI: 10.1039/D0RA01479F
[30] Faisal S, Al-Radadi NS, Jan H, Abdullah, Shah SA, Shah S, et al. Curcuma longa mediated synthesis of copper oxide, nickel oxide and Cu-Ni bimetallic hybrid nanoparticles: Characterization and evaluation for antimicrobial, anti-parasitic and cytotoxic potentials. Coatings, 2021, 11(7), 849. DOI: 10.3390/coatings11070849
[31] Fathi MR, Asfaram A, Farhangi A. Removal of Direct Red 23 from aqueous solution using corn stalks: isotherms, kinetics and thermodynamic studies. Spectrochimica Acta Part A: Molecular and Biomolecular Spectroscopy, 2015, 135, 364-372. DOI: 10.1016/j.saa.2014.07.008
[32] Erbil K. Malachite green adsorption onto modified pine cone: Isotherms, kinetics and thermodynamics mechanism. Chemical Engineering Communications, 2021, 208(3), 318-327. DOI: 10.1080/00986445.2020.1715961

[33] Alameri AA, Alfilh RHC, Awad SA, Zaman GS, Al-Musawi TJ, Joybari MM, et al. Ciprofloxacin adsorption using magnetic and ZnO nanoparticles supported activated carbon derived from *Azolla filiculoides* biomass. Biomass Conversion and Biorefinery, 2024, 14(21), 27001-27014. DOI: 10.1007/s13399-022-03372-6

[34] Fiyadh SS, AlOmar MK, Binti Jaafar WZ, AlSaadi MA, Fayaed SS, Binti Koting S, et al. Artificial neural network approach for modelling of mercury ions removal from water using functionalized CNTs with deep eutectic solvent. International Journal of Molecular Sciences, 2019, 20(17), 4206. DOI: 10.3390/ijms20174206

[35] Hosain ANA, El Nemr A, El Sikaily A, Mahmoud M.E, Amira MF. Surface modifications of nanochitosan coated magnetic nanoparticles and their applications in Pb(II), Cu(II) and Cd(II) removal. Journal of Environmental Chemical Engineering, 2020, 8 (5), 104316. DOI: 10.1016/j.jece.2020.104316

[36] El Malti W, Hijazi A, Abou Khalil Z, Yaghi Z, Medlej MK, Reda M. Comparative study of the elimination of copper, cadmium, and methylene blue from water by adsorption on the citrus Sinensis peel and its activated carbon. RSC Advances, 2022, 12(17), 10186-10197. DOI: 10.1039/D1RA08997H

[37] Sudarni DHA, Aigbe UO, Ukhurebor KE, Onyancha RB, Kusuma HS, Darmokoesoemo H, et al. Malachite green removal by activated potassium hydroxide clove leaf agrowaste biosorbent: characterization, kinetic, isotherm, and thermodynamic studies. Adsorption Science & Technology, 2021, 2021, 1145312. DOI: 10.1155/2021/1145312

[38] Chanzu HA, Onyari JM, Shiundu PM. Brewers' spent grain in adsorption of aqueous congo red and malachite green dyes: batch and continuous flow systems. Journal of Hazardous Materials, 2019, 380, 120897. DOI: 10.1016/j.jhazmat.2019.120897

[39] Zhao SX, Ta N, Wang XD. Effect of temperature on the structural and physicochemical properties of biochar with apple tree branches as feedstock material. Energies, 2017, 10(9), 1293. DOI: 10.3390/en10091293

[40] Mohammed AA, Najim AA, Al-Musawi TJ, Alwared AI. Adsorptive performance of a mixture of three nonliving algae classes for nickel remediation in synthesized wastewater. Journal of Environmental Health Science and Engineering, 2019, 17(2), 529-538. DOI: 10.1007/s40201-019-00367-w

[41] Wattanakornsiri A, Rattanawan P, Sanmueng T, Satchawan S, Jamnongkan T, Phuengphai P. Local fruit peel biosorbents for lead(II) and cadmium(II) ion removal from waste aqueous solution: A kinetic and equilibrium study. South African Journal of Chemical Engineering, 2022, 42, 306-317. DOI: 10.1016/j.sajce.2022.09.008

[42] Wang D, Zhang J, Guo L, Dong X, Shen H, Fu F. Synthesis of nano-porous $Bi_2WO_6$ hierarchical microcrystal with selective adsorption for cationic dyes. Materials Research Bulletin, 2016, 83, 387395. DOI: 10.1016/j.materresbull.2016.06.029.

[43] Kumar PS, Saravanan A, Rajan PS, Yashwanthraj M. Nanoscale zero-valent iron-impregnated agricultural waste as an effective biosorbent for the removal of heavy metal ions from wastewater. Textiles and Clothing Sustainability, 2016, 2(1), 3. DOI: 10.1186/s40689-016-0014-5

[44] Giri BS, Sonwani RK, Varjani S, Chaurasia D, Varadavenkatesan T, Chaturvedi P, et al. Highly efficient bio-adsorption of Malachite green using Chinese Fan-Palm Biochar (Livistona chinensis). Chemosphere, 2022, 287, 132282. DOI: 10.1016/j.chemosphere.2021.132282.

[45] Umeh CT, Nduka JK, Akpomie KG, Ighalo JO, Mogale R. Adsorptive effect of corn silk-loaded nickel oxide and copper oxide nanoparticles for elimination of ciprofloxacin from wastewater. ACS Omega, 2025, 10(4), 3784-3800. DOI: 10.1021/acsomega.4c09192

[46] Velić N, Stjepanović M, Pavlović S, Bagherifam S, Banković P, Jović-Jovičić N. Modified lignocellulosicwaste for the amelioration of water quality: adsorptive removal of congo red and nitrate using modified poplar sawdust. Water, 2023, 15(21), 3776. DOI: 10.3390/w15213776

[47] Saravana A, Kumar PS, Hemavathy RV, Jeevanantham S, Harikumar P, Priyanka G, et al. A comprehensive review on sources, analysis and toxicity of environmental pollutants and its removal methods from water environment. Science of Total Environment, 2022, 812, 152456. DOI: 10.1016/j.scitotenv.2021.152456

[48] Takdastan A, Samarbaf S, Tahmasebi Y, Alavi N, Babaei AA. Alkali modified oak waste residues as a cost-effective adsorbent for enhanced removal of cadmium from water: Isotherm, kinetic, thermodynamic and artificial neural network modeling, Journal of Industrial and Engineering Chemistry, 2019, 78, 352-363. DOI: 10.1016/j.jiec.2019.05.034

[49] Umeh CT, Nduka JK, Refilwe M, Akpomie G K, Okoye NH. Acid activated corn silk as a promising phytosorbent for uptake of malachite green and Cd (II) ion from simulated wastewater: Equilibrium, kinetic and thermodynamic studies. International Journal of Phytoremediation, 2024, 26(10), 1593-1610. DOI: 10.1080/15226514.2024.2339478

[50] Naghizadeh A. Regeneration of carbon nanotubes exhausted with humic acid using electro-Fenton technology. Arabian Journal of Science and Engineering, 2016, 41(1), 155-161. DOI: 10.1007/s13369-015-1643-8